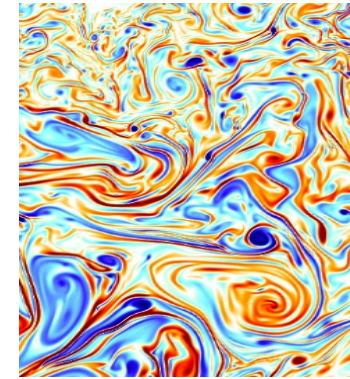
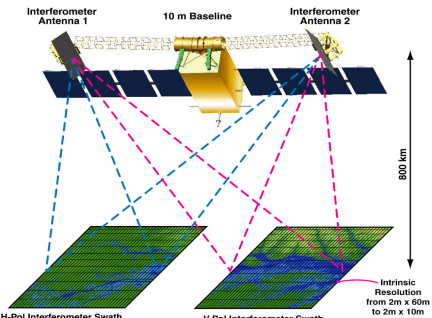


"Ocean Turbulence from SPACE"

Patrice Klein (Caltech/JPL/Ifremer)

(VII) - 2-D Turbulence (c)

[Direct enstrophy cascade, tracer and particles dispersion,
Lyapunov exponents]



**Direct cascade of enstrophy (or tracer variance)
in a turbulent geophysical flow
(using 2-D framework)**

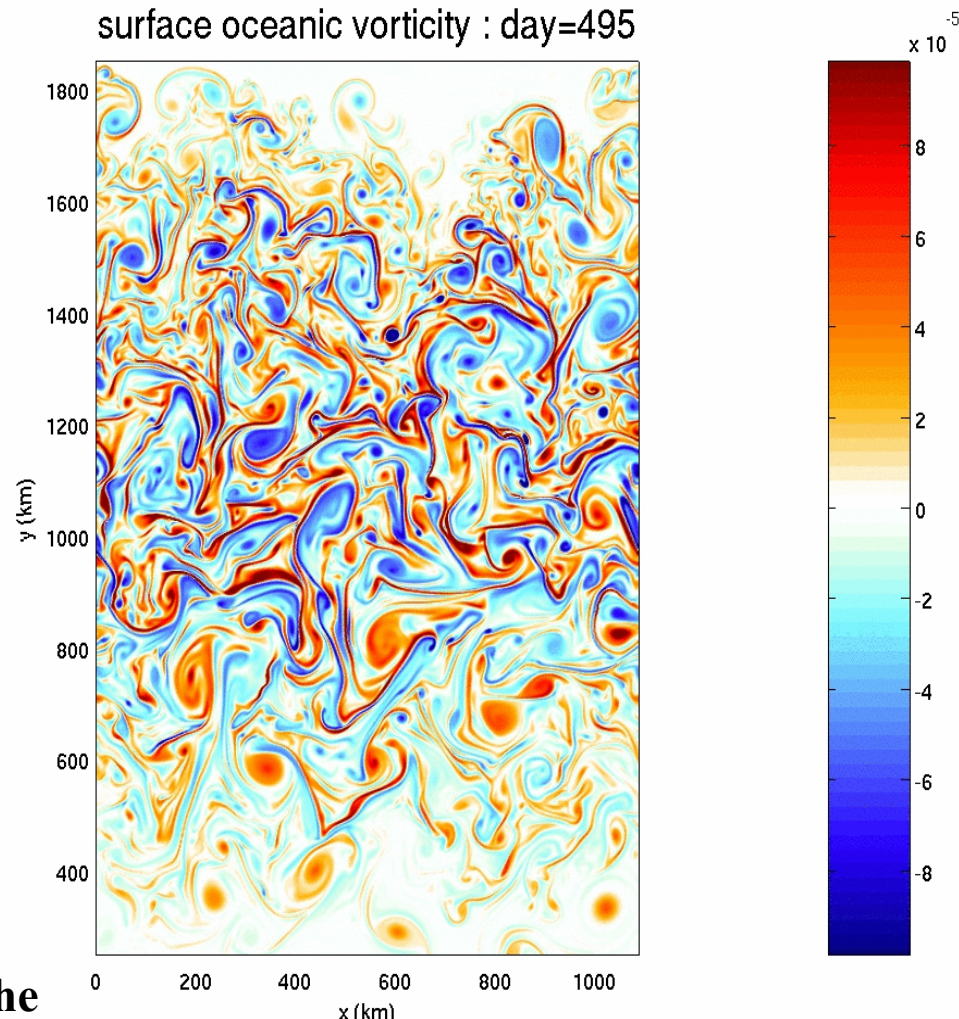
Simulation of eddy turbulence

*PE model 1/100e degree, 200 levels
[3000km*2000km*4000m]*

**Eddy turbulent field near the surface:
Vorticity field is quickly evolving.**

Direct cascade of enstrophy concerns the emergence of small-scale structures that are ultimately dissipated.

The mechanisms are the same as for the direct cascade of the variance of any tracer.



To understand the mechanisms that drive the direct cascade of tracer variance, go back again to the Euler equations ...

Two dimensional turbulence

$$\mathbf{U} = (u, v).$$

$$\nabla \cdot \mathbf{U} = 0$$

Euler equations

$$\frac{\partial u}{\partial t} + \mathbf{U} \cdot \nabla u - (f_0 + \beta y) v = -\frac{1}{\rho_0} \frac{\partial p}{\partial x} + [\text{mixing}],$$

$$\frac{\partial v}{\partial t} + \mathbf{U} \cdot \nabla v + f_0 + \beta y) u = -\frac{1}{\rho_0} \frac{\partial p}{\partial y} + [\text{mixing}].$$

In 2-D flow we can define a stream function ψ :

$$u = -\psi_y \quad v = \psi_x$$

We use $\tilde{p} = \frac{p}{\rho_0} - (f_0 + \beta y) \psi$

\tilde{p}

$$\Rightarrow \frac{\partial u}{\partial t} + \mathbf{U} \cdot \nabla u = -\frac{\partial \tilde{p}}{\partial x} + [\text{mixing}]$$

$$\frac{\partial v}{\partial t} + \mathbf{U} \cdot \nabla v = -\frac{\partial \tilde{p}}{\partial y} - \beta \psi + [\text{mixing}].$$

Vorticity eq.

$$\zeta = v_x - u_y$$

$$\frac{\partial \zeta}{\partial t} + \mathbf{U} \cdot \nabla \zeta + \beta u = 0.$$

Divergence eq.

$$\nabla \cdot [\mathbf{U} \cdot \nabla \psi] = - \Delta \tilde{p} + \beta u$$

Note that:

$$\nabla \cdot [\mathbf{U} \cdot \nabla \psi] = \frac{1}{2} w = \frac{1}{2} [S_1^2 + S_2^2 - \zeta^2]$$

$$\text{with } S_1 = u_x - v_y = 2u_x, \quad S_2 = u_x + u_y$$

w is the Okubo - Weis criterion $w = [S_1^2 + S_2^2 - \zeta^2]$.

[See Okubo (DSR 1970) and Weis. (1981 (Report Scrips) and 1991 (Physical).)]

w is related to second-order derivatives of ψ and therefore to the ψ -curvature.

W partitions the stream function ψ into hyperbolic and elliptic regions

KE and Z cascades

In 2-D turbulence both KE and Z are conserved. Because of these two invariants, there is:

- a KE transfer from small to larger scales,
- **a Z transfer from large to smaller scales,**

These transfers occur through the nonlinear terms.

What are the mechanisms that drive the direct cascade of enstrophy and tracer variance?

$$\mathcal{W} = (u, v) = (-\psi_y, \psi_x)$$

$$\frac{\partial \zeta}{\partial t} + \mathcal{W} \cdot \nabla \zeta + \cancel{\rho \nu} = 0. \quad \text{with } \zeta = v_x - u_y.$$

Let us consider a tracer (as the vorticity) conserved on a Lagrangian trajectory

$$\frac{\partial C}{\partial t} + \mathcal{W} \cdot \nabla C = 0. \quad \text{or} \quad \frac{dC}{dt} = 0$$

Time evolution for the tracer gradient, ∇C , is:

$$\frac{d \nabla C}{dt} = -[\nabla \mathcal{W}]^T \nabla C \quad \text{with } [\nabla \mathcal{W}]^T = \begin{bmatrix} u_x & v_x \\ u_y & v_y \end{bmatrix} \text{ and } \nabla C = \begin{bmatrix} c_x \\ c_y \end{bmatrix}$$

$$\text{Note that } [\nabla \mathcal{W}]^T = \frac{1}{2} \begin{bmatrix} s_1 & s_2 + \zeta \\ s_2 - \zeta & -s_1 \end{bmatrix} \quad \text{with } s_1 = u_x - u_y = 2u_x, s_2 = v_x + v_y$$

The eigenvalues of $[\nabla \mathcal{W}]^T$ are:

$$\lambda_0 = \pm \frac{1}{2} [s_1^2 + s_2^2 - \zeta^2]^{1/2} = \pm \frac{1}{2} [\mathcal{W}]^{1/2}$$

Assuming the flow is slowly varying with respect to the tracer gradients, the solution becomes:

$$\nabla C(t) \approx \nabla C(t=0) \exp \left[\pm \lambda_0 t \right]$$

Solutions:

1] If $d_0^2 (= \frac{\omega}{4}) > 0$ the strain dominates and d_0 is real.

Solutions are:

$$\nabla G(t) \approx \begin{bmatrix} e^{\pm d_0 t} & 0 \\ 0 & e^{\mp d_0 t} \end{bmatrix} \cdot \nabla G(t=0)$$

An exponential growth in one direction and exponential decay in the other. The directions are given by the eigenvectors.

2] If $d_0^2 (= \frac{\omega}{4}) < 0$ the vorticity dominates and d_0 is pure imaginary.

$$\rightarrow \nabla G(t) \approx \exp[\pm i d_0 t] \cdot \nabla G(t=0).$$

No growth. Just a rotation

3] If $d_0^2 (= \frac{\omega}{4}) = 0$. This corresponds to regions such as in a current shear (for example $U_y \neq 0$, $U_x = U_z = 0$).

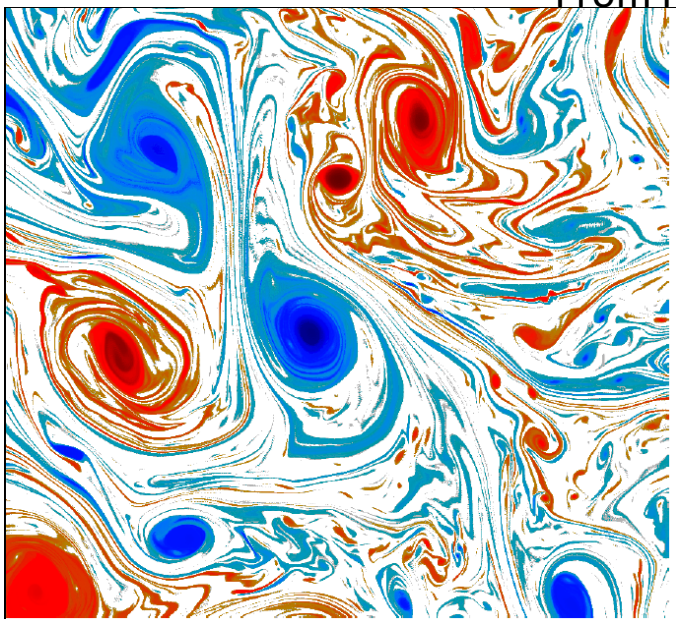
For this example solutions are:

$$\nabla C(t) = \begin{bmatrix} C_x(t) \\ C_y(t) \end{bmatrix} = \begin{bmatrix} C_x(t=0) \\ U_y t + C_y(t=0) \end{bmatrix}$$

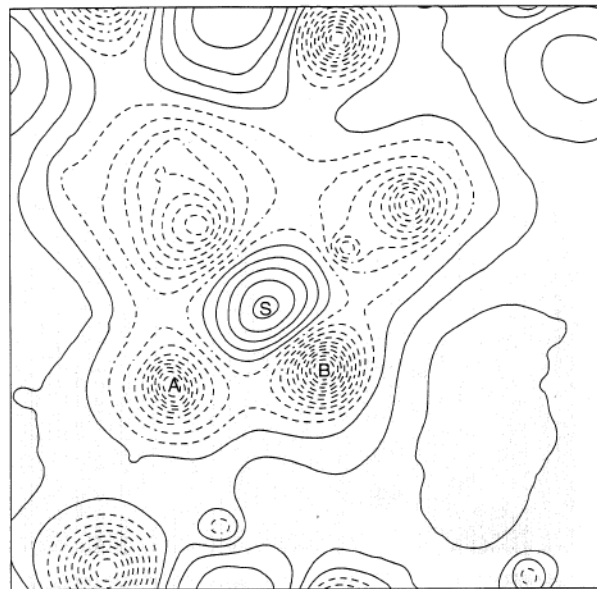
There is a linear growth

So tracer gradients either grow (exponentially or linearly) or rotate.

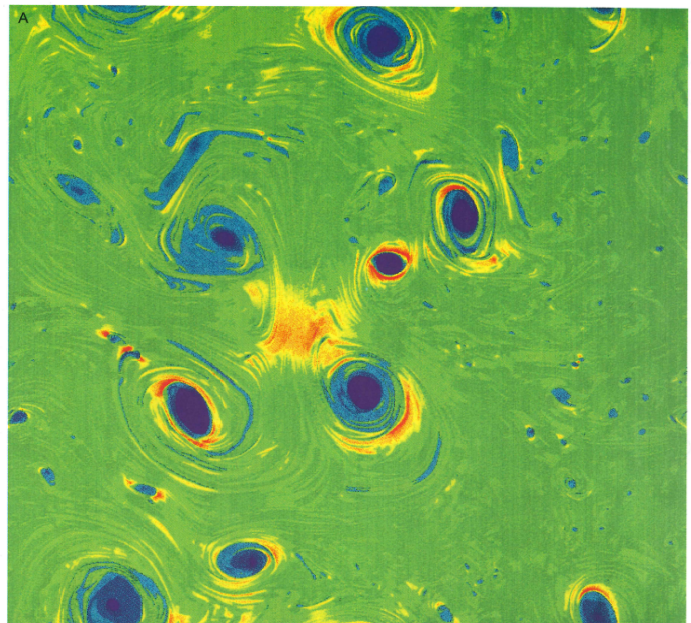
These solutions assume that $[\nabla U]^T$ is slowly varying.



$\leftarrow \zeta$

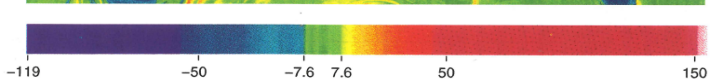


$\leftarrow \tilde{p}$



$$\lambda_o^2 = \frac{W}{4} = -\frac{\Delta \tilde{p}}{2}$$

The total area of regions with significant positive values (stirring regions) of W is small compared to the total area of the vortices (no tracer gradient growth)



Previous solutions, based only on \mathbf{W} , assume that

$[\nabla U]^T$ (and therefore \mathbf{W}) is slowly varying.

Is it true ?

This assumption can be inspected by looking at the second-order derivative:

$$\frac{d^2 \nabla C}{dt^2} = -[\nabla U]^T \cdot \underbrace{\frac{d \nabla C}{dt}}_{T_C} - \underbrace{\frac{d}{dt} [\nabla U]^T}_{T_U} \cdot \nabla C = \left[[\nabla U]^T^2 - \frac{d [\nabla U]^T}{dt} \right] \cdot \nabla C.$$

If $T_U \gg T_C$ then $\frac{d [\nabla U]^T}{dt} \cdot \nabla C \ll [\nabla U]^T \cdot \frac{d \nabla C}{dt}$.
Is this true?

We have to come back to the Euler equations to check.

$$\begin{aligned} \dot{Y}_u &= \frac{du}{dt} = -\tilde{p}_x & \dot{Y}_v &= \frac{dv}{dt} = -\tilde{p}_y \\ \Rightarrow \frac{d \zeta}{dt} &= 0, \quad \frac{d S_1}{dt} = -(\tilde{p}_{xx} - \tilde{p}_{yy}), \quad \frac{d S_2}{dt} = -2\tilde{p}_{xy} \end{aligned}$$

$$\Rightarrow \frac{d [\nabla U]^T}{dt} = \frac{1}{2} \begin{bmatrix} -[\tilde{p}_{xx} - \tilde{p}_{yy}] & -2\tilde{p}_{xy} \\ -2\tilde{p}_{xy} & [\tilde{p}_{xx} - \tilde{p}_{yy}] \end{bmatrix}$$

$$[\nabla U^T]^2 = \frac{1}{4} \begin{bmatrix} S_1^2 + S_2^2 - \zeta^2 & 0 \\ 0 & S_1^2 + S_2^2 - \zeta^2 \end{bmatrix} = -\frac{1}{2} \begin{bmatrix} \tilde{p}_{xx} + \tilde{p}_{yy} & 0 \\ 0 & \tilde{p}_{xx} + \tilde{p}_{yy} \end{bmatrix}$$

$$\text{using } \omega = S_1^2 + S_2^2 - \zeta^2 = -2\Delta\tilde{p}$$

$$\Rightarrow [\nabla U^T]^2 - \frac{d [\nabla U]^T}{dt} = - \begin{bmatrix} \tilde{p}_{xx} & \tilde{p}_{xy} \\ \tilde{p}_{xy} & \tilde{p}_{yy} \end{bmatrix} = [\nabla \gamma] !$$

The eigenvalues of $[\nabla U]^T - \frac{d}{dt} [\nabla U]^T = - \begin{bmatrix} \hat{p}_{xx} & \hat{p}_{xy} \\ \hat{p}_{yx} & \hat{p}_{yy} \end{bmatrix}$ are:

$$\lambda_{\pm} = \underbrace{-\frac{(\hat{p}_{xx} + \hat{p}_{yy})}{2}}_{w/y.}, \quad \underbrace{\pm \sqrt{\left(\hat{p}_{xx} - \hat{p}_{yy}\right)^2 + (2\hat{p}_{xy})^2}}_{\lambda_1}$$

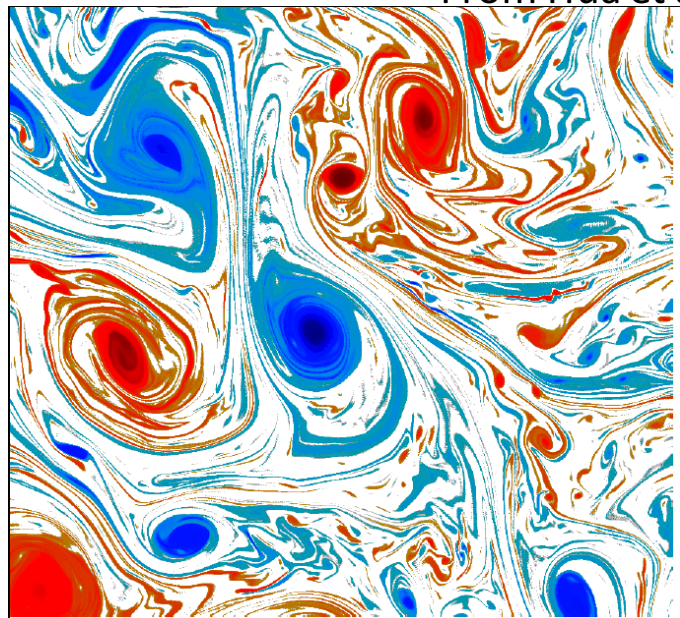
$$\Rightarrow \nabla G(t) \approx \nabla G(t=0) \cdot \exp [\pm (\lambda_{\pm})^{1/2} t]$$

The \hat{p} field (as the Ψ field) can be decomposed into elliptic and hyperbolic regions.

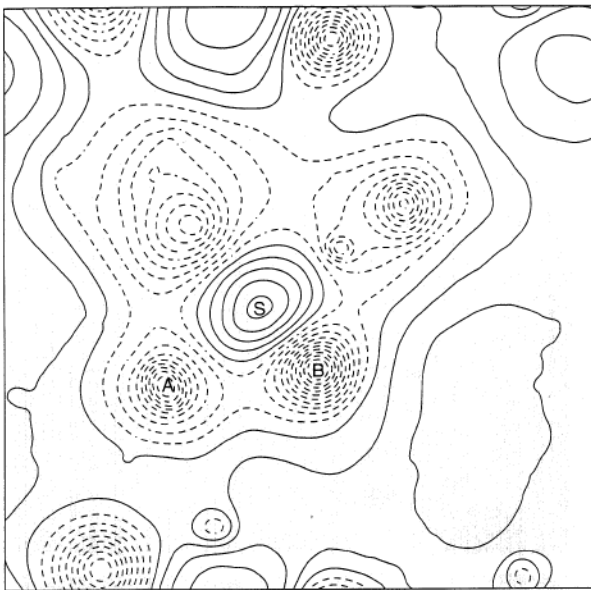
- Elliptic regions correspond to large values of $|\Delta \hat{p}|$.
- Hyperbolic regions " " " " " of $(\hat{p}_{xx} - \hat{p}_{yy})^2 + 4\hat{p}_{xy}^2$

So, the assumption of $[\nabla U]^T$ slowly varying. is valid in elliptic \hat{p} regions but NOT in hyperbolic \hat{p} -regions.

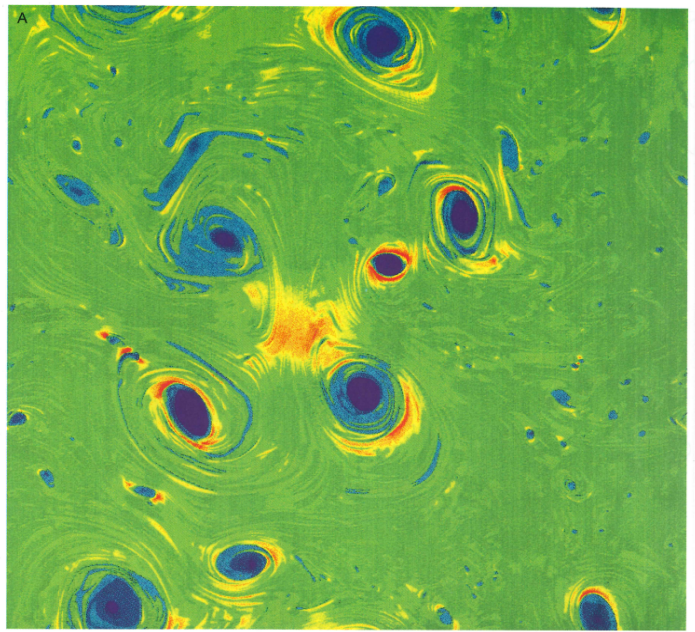
Check with numerical simulations --



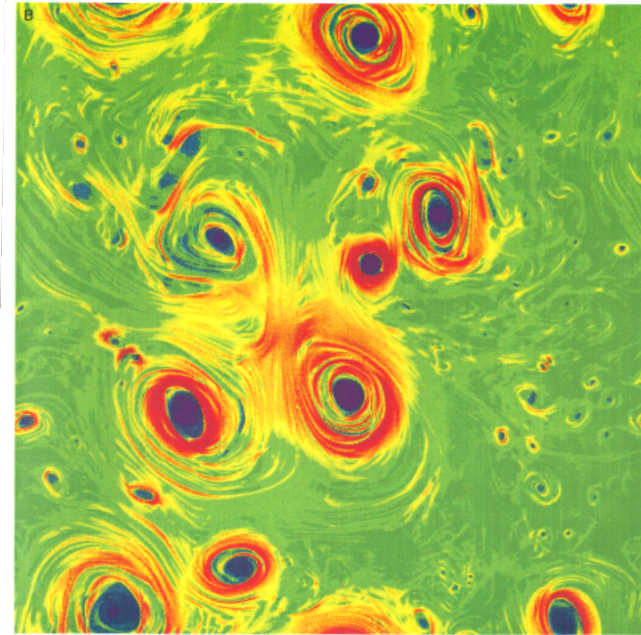
ζ



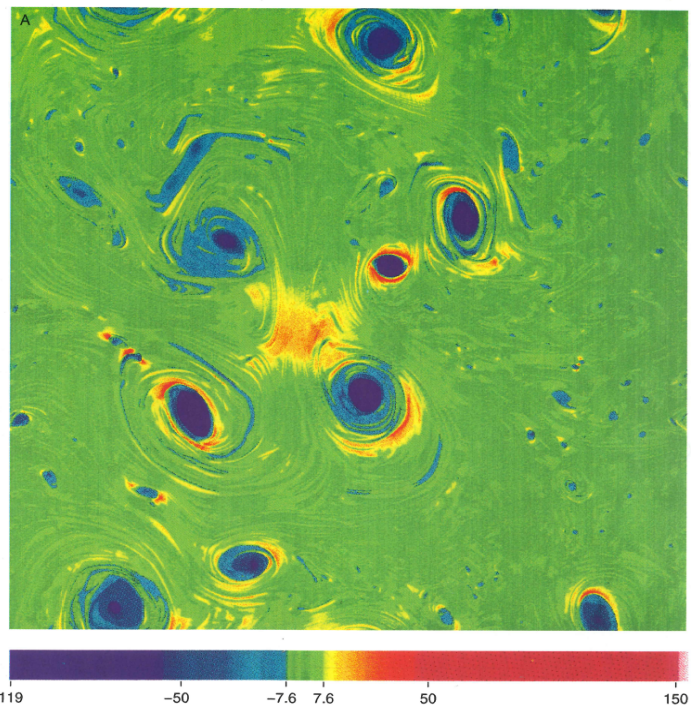
\tilde{p}



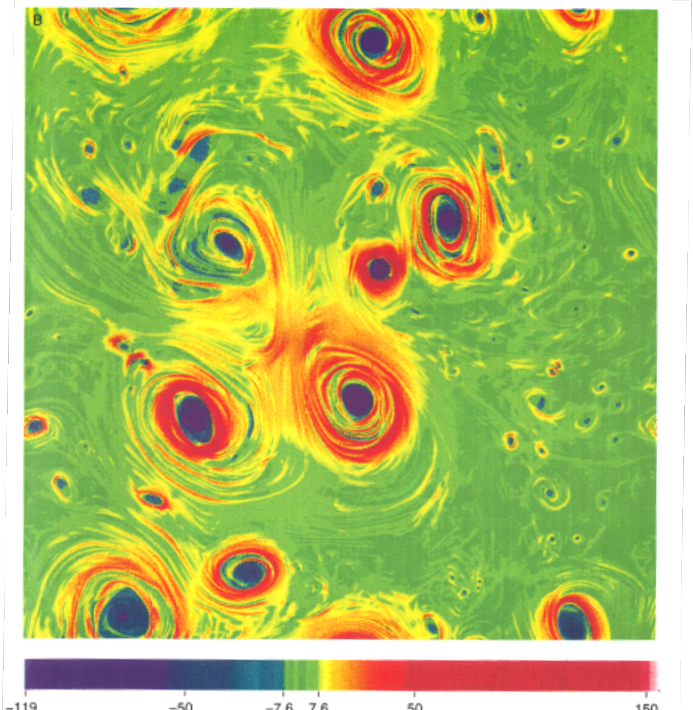
$$W/4 = -\frac{1}{2} \Delta \tilde{p}$$



$$\lambda_+ = -\frac{1}{2} \Delta \tilde{p} + \frac{1}{2} \sqrt{\{(\tilde{p}_{xx} - \tilde{p}_{yy})^2 + 4\tilde{p}_{xy}^2\}}$$



$W/4 = \frac{1}{2} \Delta \tilde{p}$

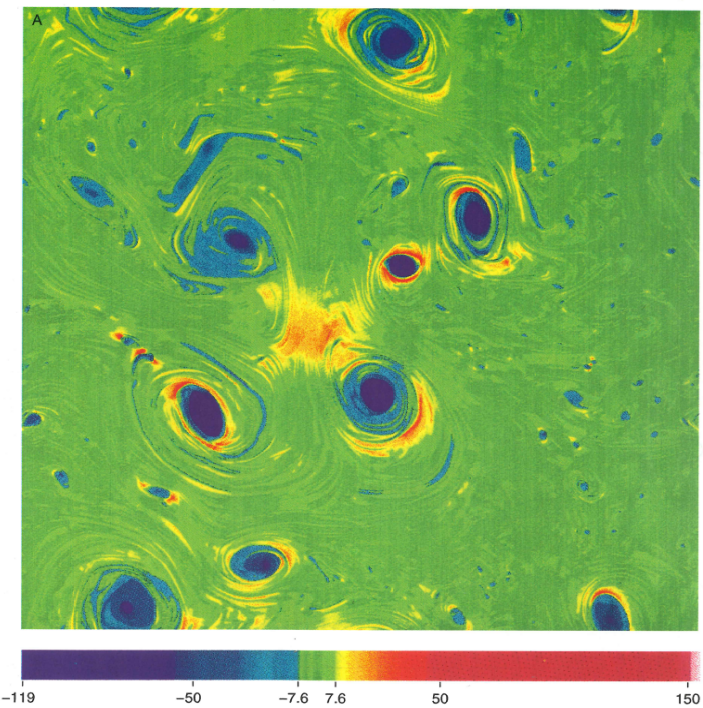


$$\lambda_+ = -\frac{1}{2} \Delta \tilde{p} + \frac{1}{2} \sqrt{\{(\tilde{p}_{xx} - \tilde{p}_{yy})^2 + 4\tilde{p}_{xy}^2\}}$$

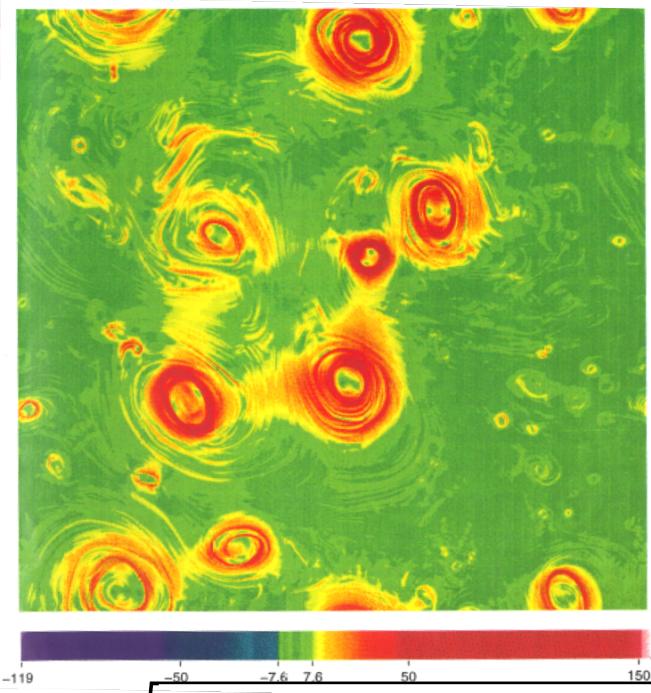
Regions of λ_+ with significant positive values are much broader than those for $W/4$, in particular around the vortices.

This is due to the time variation of ∇U in these regions (that correspond to the departure of the \tilde{p} field from an axisymmetric pattern and to hyperbolic regions of the \tilde{p} field).

See the λ_1 field ...



$W/4 = \frac{1}{2} \Delta \tilde{p}$



$$\lambda_1 = \frac{1}{2} \sqrt{\{(\tilde{p}_{xx} - \tilde{p}_{yy})^2 + 4\tilde{p}_{xy}^2\}}$$

Regions of λ_1 with significant positive values are located around vortices and near the saddle points of close vortices.

The direct cascade of tracer variance (or enstrophy) is much more efficient than diagnosed from the Okubo-Weiss criterion alone ! Stirring processes are entirely governed by $[\nabla \gamma]$

These results highlight the production of strong tracer (or vorticity) gradients around the vortices. These gradients are usually transport barriers (or dynamical barriers)!

The results highlight the physical mechanisms involved in the transfer of tracer (or vorticity) variance from large to smaller scales as sketched by the simple analysis discussed in the previous class. **Stirring is directly related to the geometry of the pressure field** and not from that of the streamfunction.

Note that the Okubo-Weiss quantity (deduced from the velocity field) allows to get the pressure field.

One way to visualize the tracer cascade is to integrate the tracer equation. Another way is to consider the particle dispersion evolution to get the **Lyapunov exponents**. We just need to know the surface velocity field and its evolution in time.

It is now common for many applied problems (such as oil spills, dispersion of pollutants and biogeochemical transport) to make use of Lyapunov exponents

First it can be shown that the **particle dispersion is driven by the same mechanisms as those that affect the tracer gradients**.

The argument is the following ...

Particle dispersion: a dual problem

[see Lapeyre, Chaos 2002]

Using $X = \begin{bmatrix} x \\ y \end{bmatrix}$ and $\frac{dX}{dt} = U(X)$ with $U = (u, v)$,

we consider $\delta X = \begin{bmatrix} \delta x \\ \delta y \end{bmatrix}$ the vector separating two particles initially close. From a Taylor expansion we get:

$$\frac{d\delta X}{dt} = [\nabla U] \delta X \quad (\text{II-1}) \quad \text{with } [\nabla U] = \begin{bmatrix} u_x & u_y \\ v_x & v_y \end{bmatrix}$$

Properties of the particle dispersion can be directly related to the properties of the tracer cascade.

If C_1 and C_2 are the tracer magnitudes for two particles separated by the vector δX , then a Taylor series expansion leads to:

$$\delta C = C_1 - C_2 \approx \nabla G^T \cdot \delta X$$

Since G is conserved on a Lagrangian trajectory, we have:

$$\frac{d}{dt} [\nabla G^T \cdot \delta X] = 0 \quad (\text{II-2})$$

which leads (using II-1) to:

$$\frac{d \nabla G^T}{dt} = - \nabla G^T \cdot [\nabla U] \quad \text{or} \quad \frac{d \nabla G}{dt} = - [\nabla U]^T \nabla G \quad (\text{II-3})$$

Lyapunov exponents:

A common way to characterize the particle dispersion (or the tracer dispersion) is to use Lyapunov exponents.

The method consists of considering initially a quasi-uniform distribution of particles in the flow domain and to advect them in time with the observed velocity field.

If $\delta X(t_1)$ is the vector separating two particles at time t_1 , the Lyapunov exponent, μ , is defined as:

$$\mu = \lim_{t_2 \rightarrow \infty} \frac{1}{t_2 - t_1} \log \left[\frac{|\delta X(t_2)|}{|\delta X(t_1)|} \right]$$

Coming back to the equation for the particle dispersion:

$$\frac{d\delta X}{dt} = [\nabla U] \cdot \delta X,$$

Solution is:

$$\delta X(t) \approx \delta X(t_1) \cdot e^{\pm \lambda t}$$

which leads to:

$$\mu \approx \lambda$$

Finite Size Lyapunov Exponents (FSLE):

A practical Lyapunov exponent used in atmospheric and oceanic flows is the FSLE.

If we consider a pair of particles initially separated by δ_o at position x and time t , the FSLE is expressed as the time τ it takes for the pair of particles to be separated by a given distance δ_j . Its expression is:

$$\mu(x, t, \delta_o, \delta_j) = \frac{1}{\tau} \log \left[\frac{\delta_j}{\delta_o} \right]$$

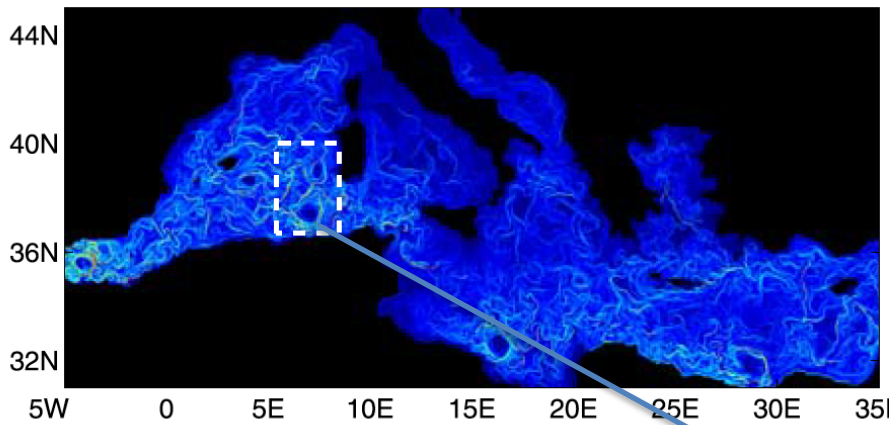
The FSLE depends on the choice of δ_o and δ_j .

Practically the field is initialized with a quasi-uniform distribution of N particles. Then we consider a slightly perturbed distribution of another set of N particles (by a distance of δ_o from the original distribution), which generates a pair of N particles.

Particles are advected **forward** in time using the observed velocity field. This allows to get $\mu_+(x, t, \delta_o, \delta_j) = \frac{1}{\tau} \log \left[\frac{\delta_j}{\delta_o} \right]$ that identify the lines of **maximum stretching**.

They are also advected **backward** in time using the observed velocity field. This allows to get $\mu_-(x, t, \delta_o, \delta_j) = -\frac{1}{\tau} \log \left[\frac{\delta_j}{\delta_o} \right]$ that identify the lines of **maximum compression**.

Some first applications for the Ocean: Abraham & Bowen (Chaos, 2002), D'Ovidio et al. (GRL 2004), Waugh et al. (JPO 2006), ...



d'Ovidio et al. GRL'04

$\mu_+(x, t, \delta_o, \delta_j) > 0$: forward in time

$\mu_-(x, t, \delta_o, \delta_j) < 0$: backward in time
[units are in (day) $^{-1}$]

FSLE allow to unveil the tangle of stretching and compressing lines.

These lines also define the directions of transport of tracers.

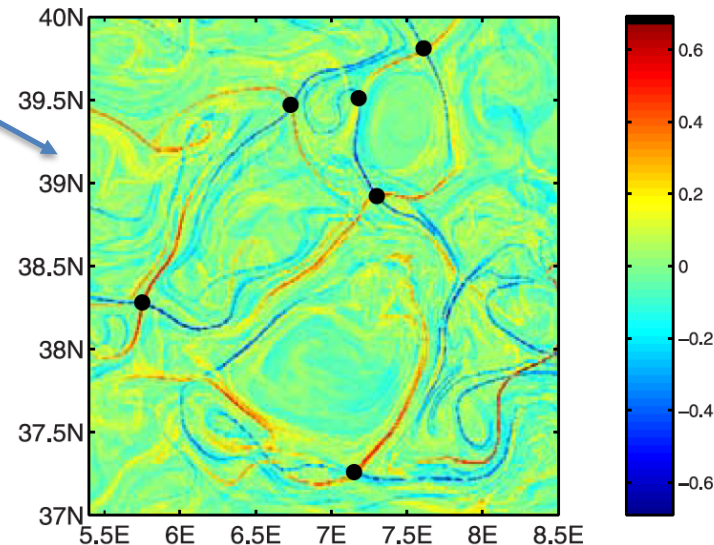
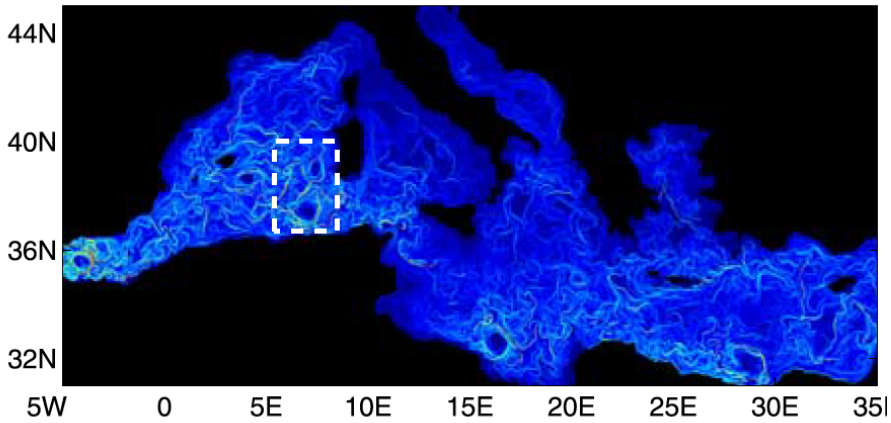


Figure 4. FSLEs calculated from forward (displayed as positive values) and backwards (displayed as negative values) integrations in time, i.e., what is plotted is the field $\lambda_+ - \lambda_-$. A region with strong mixing appears organized by a tangle of stretching and compressing manifolds. Such lines organize the flow. The black dots indicate some of the hyperbolic points that are located at the intersections of the lines.



d'Ovidio et al. GRL'04

A quantitative index of mixing in a given area, A, is the quantity:

$$M_{\pm}(t) = \langle \sqrt{\mu_+ \mu_-} \rangle_A(t)$$

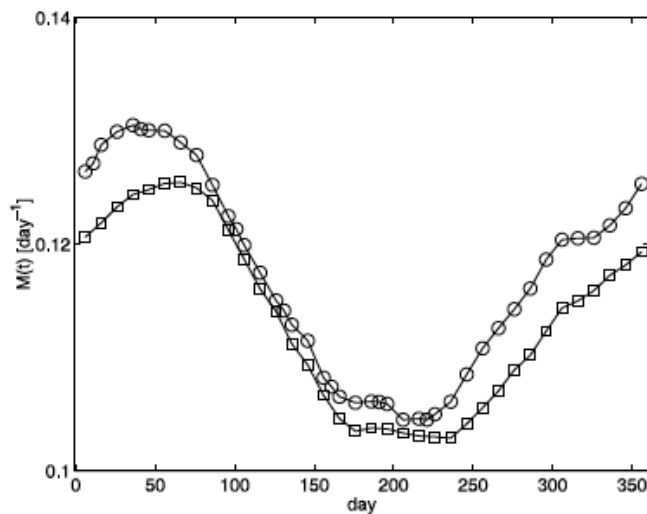
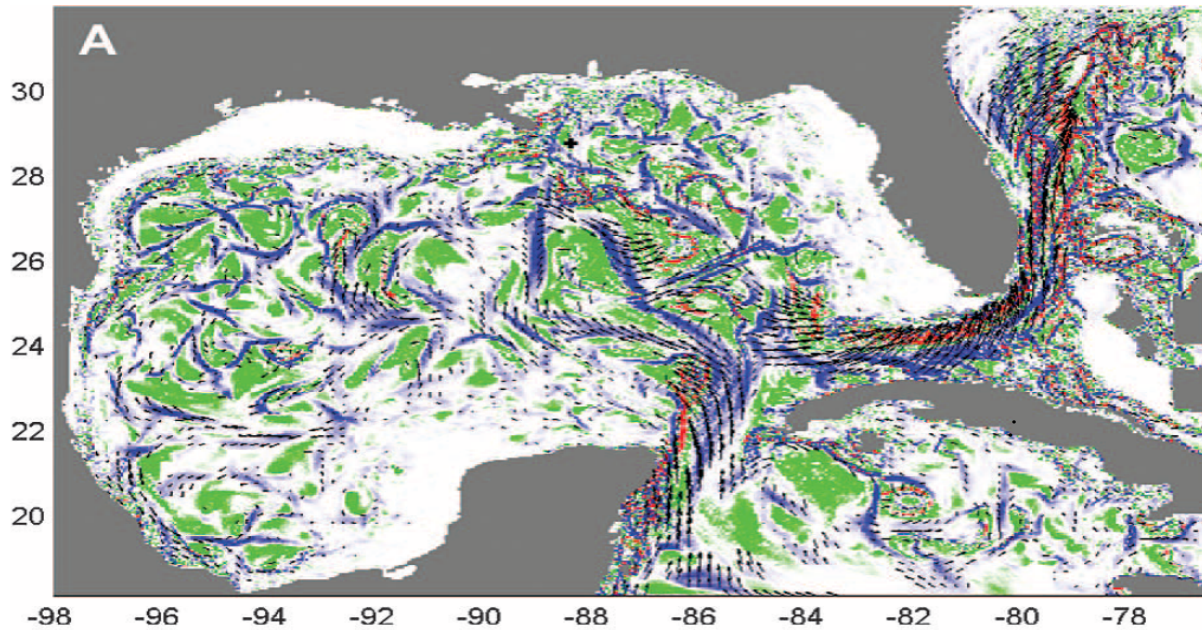


Figure 5. Temporal evolution of the mixing measures $M_+(t)$ (circles), and of $M_{\pm}(t)$ (squares) for the whole Mediterranean Sea during one simulation year. They display a very similar behavior, with maximum values in winter.

AVISO data are often used to diagnose the impact of the stirring properties of the flow field on a tracer evolution using the Lyapunov exponents.

This figure compares the forecast (blue and red colors) of the dispersion of oil spill with what was observed (in black) after the Deep Water Horizon accident in the Gulf of Mexico. This forecast is based on altimeter data.

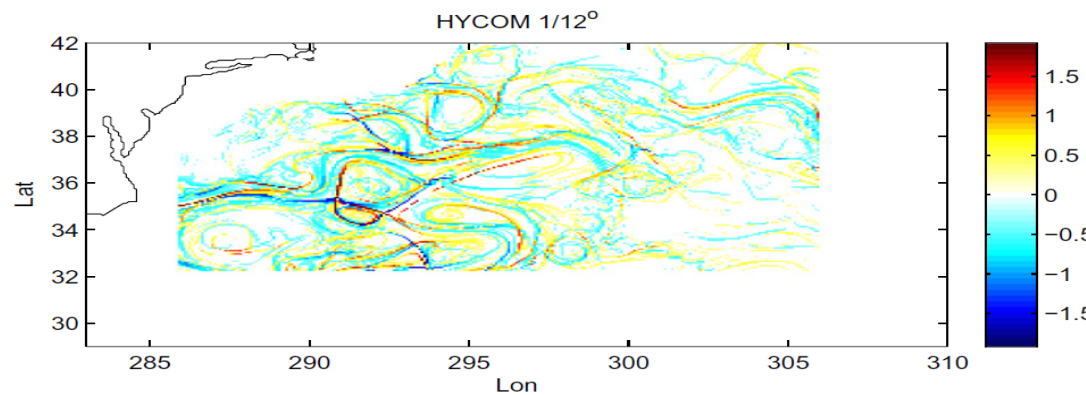


Forecast of oil spill dispersion in the Gulf of Mexico on 25 june 2010 (red and blue show regions of strong oil dispersion within 3 days), based on altimetric data. This diagnosis compared well with what was observed (Mezic et al, Science, 2010).

However ...

Impact of scales < 100 km in terms of the dispersion of pollutants or floats by the surface currents (Finite Size Lyapunov Exponents) [Haza et al. '12]

No submesoscale



With submesoscales

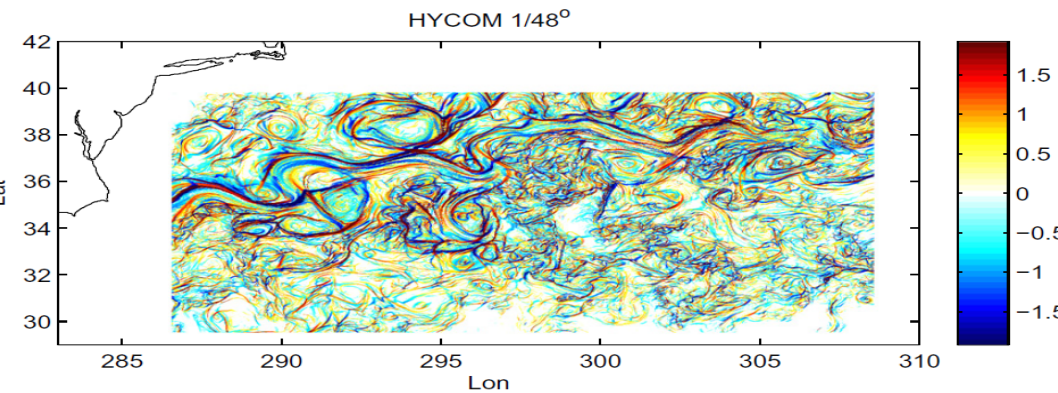


Fig. 1. FSLE branches from $1/12^\circ$ (upper panel) and $1/48^\circ$ (lower panel) HYCOM simulations in the Gulf Stream region. Note the rich submesoscale field in the higher resolution case. The color panels indicate FSLE in 1/day. Blue colors show inflowing/stable LCS from forward in time, and red colors out-flowing/unstable LCS from backward in time particle advection. (For interpretation of the references to color in this figure legend, the reader is referred to the web version of this paper.)

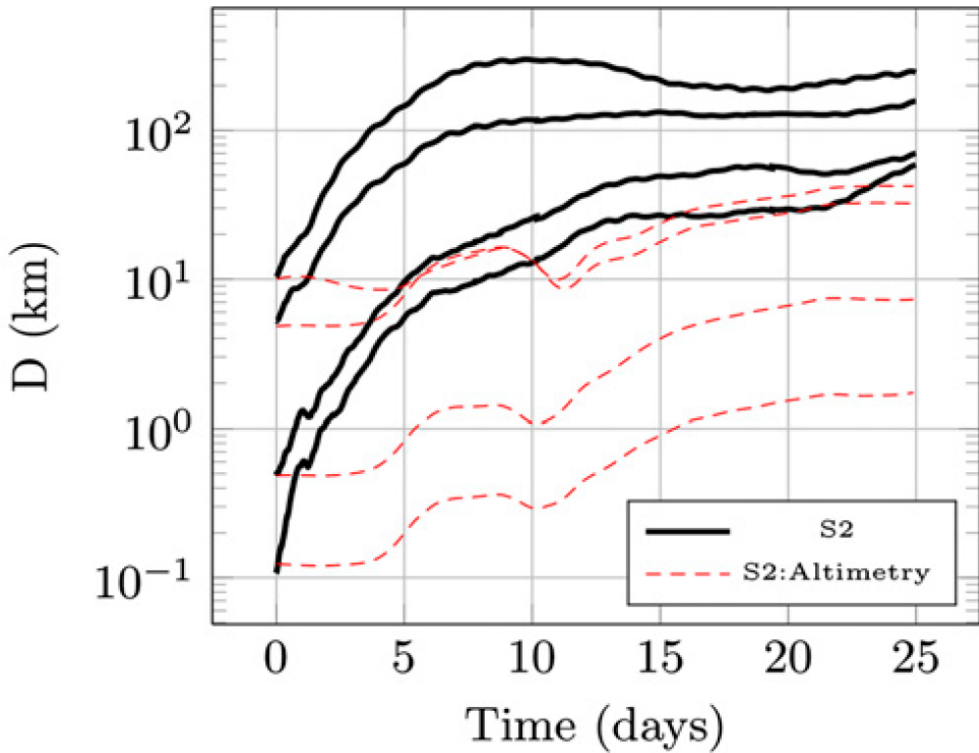
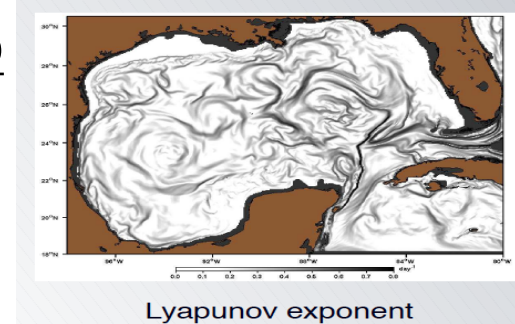
When scales < 100 km are present FSLE have a larger magnitude and involve smaller scales
=> **Dispersion by scales < 100 km is significant.**

These ideas are presently tested in the Gulf of Mexico where a very large number of surface drifters have been deployed.

Dispersion by submesoscales in the Gulf of Mexico

Separation distance of a particle pair, $D(t)$, estimated

- using HR data from 300 drifters (**black curves**): submesoscales are taken into account;
- using LR AVISO data (**red**): submesoscales are **NOT** taken into account.



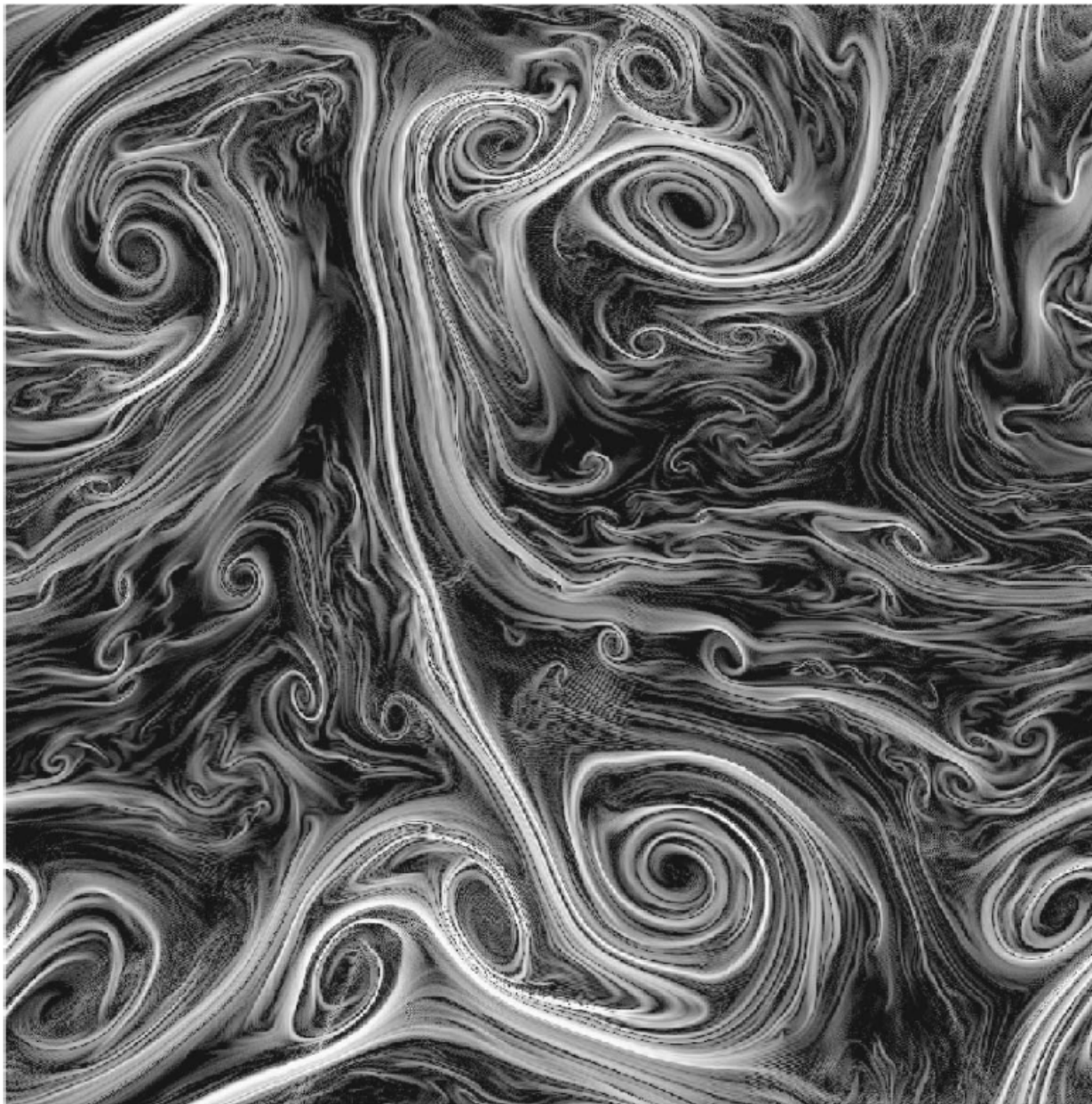
Dispersion is 10-100 times
LARGER when submesoscales
are taken into account !

(from Poje et al.'14)

What is missing in the AVISO data ?

Contribution of small scales [Ro = O(1)]!

From Lapeyre (Chaos 2002)



STIRRING VERSUS MIXING

To answer some questions asked during and after the class, here are some arguments on the competition between stirring and mixing - [see Garrett, DAO 1983 and Young et al., JPO 1982 in folder /paper/2D turbulence in the dropbox].

Eq. for the tracer gradient can be written as:

$$\frac{d \nabla C}{dt} = -[\nabla U]^T \cdot \nabla C + k_s A [\nabla C]$$

If λ is the eigenvalue of $-[\nabla U]^T$ and k_s the diffusivity, a dimensional analysis of the two R.H.S terms leads to define:

$$L_s = [k_s/\gamma]^{1/2}$$

- When L (the tracer gradient scale) $< L_s$, mixing dominates, the tracer area will increase (leading to a tracer concentration decrease) and the tracer gradient will decrease (L will increase until $L \approx L_s$)
- When $L > L_s$, stirring dominates and will increase the tracer gradient in the compression direction until $L \approx L_s$.

Using $\gamma \approx 10^{-5} s^{-1}$ $k_s = 3.6 m^2 s^{-1}$ leads to

$$L_s \approx 600 \text{ m} ?$$

$\gamma \approx 10^{-5} s^{-1}$ is a lower bound in fully turbulent flows.

$k_s \approx 3.6 \text{ m}^2 \text{s}^{-1}$ is an upper bound, [See Young et al. JPO'82 for the mechanisms leading to k_s].

From Munk et al. (2000)

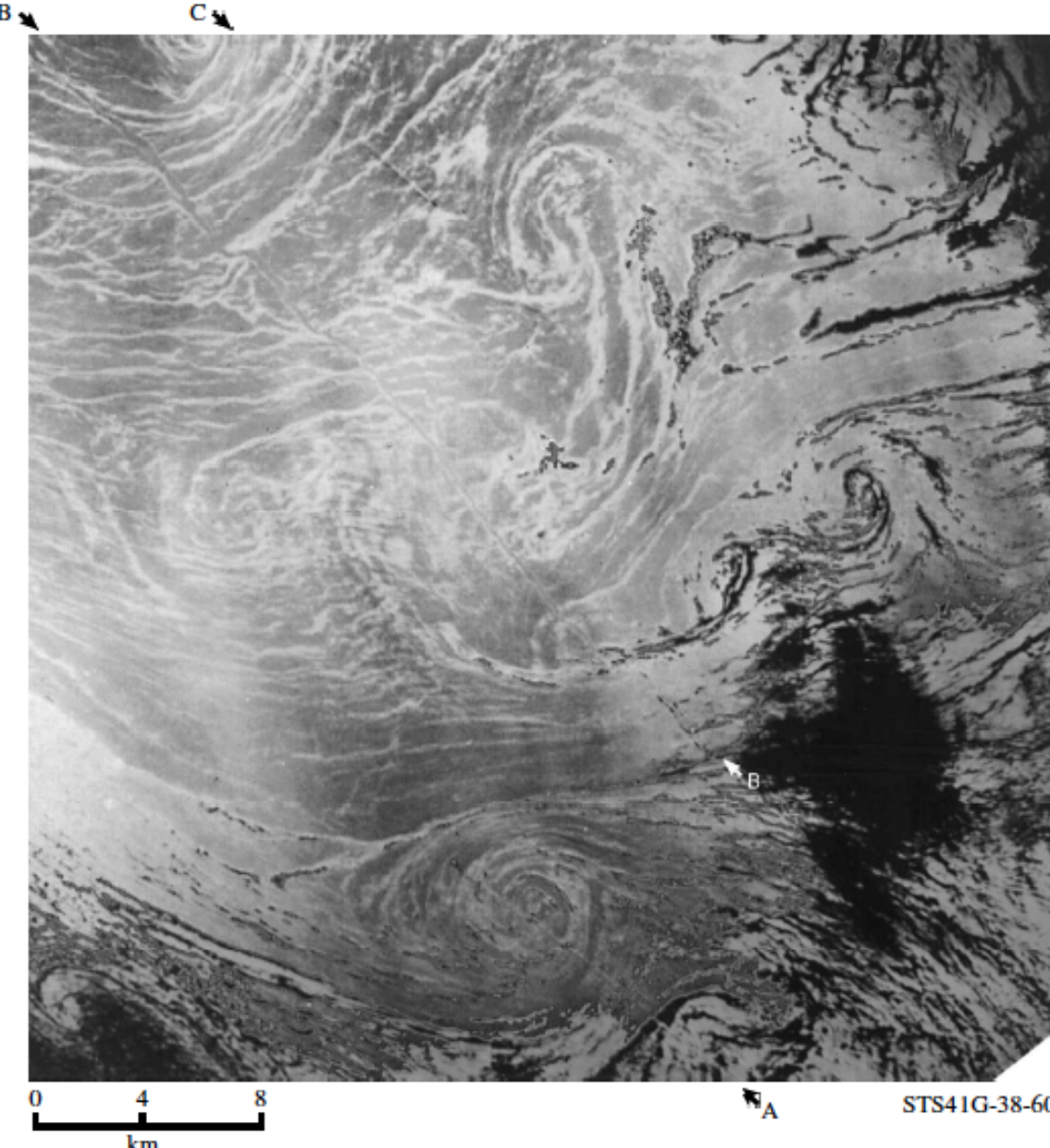


Figure 7. Ship tracks in the Ionian Sea. Tracks A and C are young with the ships visible. Track A shows minor distortion during passage through the developing core, the centre of which is ca. 3 km aft of the ship. Ship track B is old and shows significant offsets at cyclonic sharp fronts coincident with streaks. The rendition of the streaks changes from light in the inner sunlitter to the upper left, to dark in the outer sunlitter in the lower and right hand portion of the image.

